Food Anal. Methods
https://doi.org/10.1007/s12161-017-1072-2

Honey Adulteration Detection Using Raman Spectroscopy

Mircea Oroian[1] · **Sorina Ropciuc**[1] · **Sergiu Paduret**[1]

Received: 29 July 2017 / Accepted: 12 October 2017

Abstract In this study, the Raman spectroscopy was used to detect honey adulterated with fructose (F), glucose (G), inverted sugar (IS), hydrolyzed inulin syrup (IN), and malt must (M). Thus, 56 samples of authentic honeys (acacia, sunflower, tilia, polyfloral, and honeydew) and 900 adulterated samples (with 5, 10, 20, 30, 40, and 50% fructose, glucose, inverted sugar, malt must, and hydrolyzed inulin syrup) were analyzed. The classification of honey authenticity has been made using the partial least square linear discriminant analysis (PLS-LDA), and a total accuracy of 96.54% (authentic honey vs. adulterated honey) was observed, while in the case of adulterated honey, a total accuracy of 90.00% was observed, respectively. The determination of the adulterant agent concentration has been made using partial least squares regression (PLSR) and principal component regression (PCR) methods. The proposed method can be considered easy and rapid for honey adulteration detection to provide continuous in-line information.

Keywords Honey · Adulteration · Raman spectra · Statistical analysis

Introduction

Honey, a naturally sweet and levorotatory carbohydrate-rich product, is produced by honey bees and collected from the nectar of flowers (Chen et al. 2014). Natural bee honey is a unique sweetening agent that can be used by humans without processing. It is superior to other sweeteners, such as refined cane sugar, beet sugar, and maize syrup, being a valuable source of rich nutritious compounds, due to its medical benefits and unique flavor (Guelpa et al. 2016; Li et al. 2017; Zhu et al. 2010). However, honey can easily be adulterated with various cheaper sweeteners, such as refined cane sugar beet sugar, high fructose corn syrup, and maltose syrup, resulting in higher commercial profits (Li et al. 2012). Although the adulteration is done for short-term economic reasons, it can damage the interests of both producers and consumers (Chen et al. 2014).

Recently, there have been published many papers on the identification of adulterated honey using stable carbon isotopic ratio mass spectrometry (Çinar et al. 2014; Simsek et al. 2012), NIR spectroscopy (Bázár et al. 2016; Gan et al. 2015), hyper-spectral imaging (Shafiee et al. 2016), and high-performance liquid chromatography (Wang et al. 2015). These methods are time-consuming, expensive, and require a high degree of technical knowledge for data interpretation (Chen et al. 2014).

Raman spectroscopy is a spectroscopic technique used in condensed matter physics and chemistry to study vibration, rotational, and other low-frequency modes in a system. Raman spectroscopy combines the advantages of infrared spectroscopy with the advantages of near-IR spectroscopy. The advantages of Raman spectroscopy are the following: it can be used in solids and liquids as well; the sample does not require preparation; the water content does not interfere; it is a non-destructive method, highly specific to a chemical fingerprint of a material; the spectra are quickly acquired within seconds; the samples can be analyzed through glass or a polymer packaging; laser light and Raman scattered light can be transmitted by optical fibers over

✉ Mircea Oroian
m.oroian@fia.usv.ro

[1] Faculty of Food Engineering, Stefan cel Mare University of Suceava, Suceava, Romania

Published online: 23 October 2017

long distances for remote analysis; Raman spectra can be collected from a very small volume (< 1 μm in diameter); and inorganic materials are easier analyzed by Raman than by infrared spectroscopy (Owen et al. 2006).

The aim of this study was to evaluate the potential of Raman spectroscopy to distinguish the authentic honey from adulterated one, to detect the adulteration agent (e.g., glucose, fructose, inverted sugar, hydrolyzed inulin syrup, and malt must), and to determine the adulteration agent concentration using statistical analysis (partial least square linear discriminant analysis—PLS-LDA, partial least squares regression—PLSR, and principal component regression—PCR).

Materials and Methods

Samples

The samples were purchased from local beekeepers from the northeast part of Romania. The honeys (56 samples) were of different botanical origins (acacia, tilia, sunflower, honeydew, and polyfloral). Before spectral measurement, the honeys were liquefied in a water bath at 55 °C (Oroian 2012). Six honey samples of each type have been adulterated with fructose (F), glucose (G), inverted sugar (IS), hydrolyzed inulin syrup (IN), and malt must (M) in different percentages 5, 10, 20, 30, 40, and 50%, respectively.

The fructose syrup (65 °Brix) has been made using fructose (Sigma Aldrich, Germany). The glucose syrup (65 °Brix) has been made using glucose (Sigma Aldrich, Germany), but to prevent the crystallization process of the solution, the pH was corrected to 1–2 with citric acid. The inverted sugar (65 °Brix) has been made using sucrose (Sigma-Aldrich, Germany) at pH 1–2 (the solution was corrected with citric acid for the hydrolysis process). The hydrolyzed inulin syrup (65 °Brix) has been obtained by boiling inulin (Enzymes & Derivates S. A. Romania) at pH lower than 2 (the solution was corrected with citric acid for the hydrolysis process). The malt must was obtained from a local brewer factory (S.C. Bermas S. A. Romania) and concentrated till 65 °Brix.

The samples have been corrected to 65 °Brix with distilled water to avoid spectral complications from naturally occurring variations in sugar concentration (Li et al. 2012).

Raman Spectra Acquisition

The spectra were recorded using an i-Raman spectrometer (EZM-A2-785L, B&W TEK Inc., USA) equipped with a fiber-optic Raman probe, a thermoelectric cooled CCD detector with 2048 pixels and a 785-nm laser with a maximum output power of 495 mW in the signal range of 250–2339 cm^{-1} and a spectral resolution of 3 cm^{-1}. The samples were placed into a quartz cell with 1 cm path (the quartz cell is placed into a cuvette holder) scanned at an increment of 1 cm^{-1}. Integration time was of 15 s. Before being used, they were warmed up to 55 °C to dissolve any crystals and kept in flasks at 30 °C to remove air bubbles that could interfere with spectra studies (Oroian 2015).

Spectral Data Pre-treatment

In order to optimize the model (PLS-LDA, PCR, PLSR), the spectral data have been submitted to pre-treatment such as auto-scaling, mean-centering (MC), first and second derivatives, multiplicative scattering correction (MSC), airPLS, and their combination. Of all, airPLS combined with auto-scaling was the suitable model for better classification and prediction, leading to the best performance with a small number of PLS-LDA, PCR, and PLSR components. Auto-scaling equalizes variances of all variables and gives the same weight to all the variables (Li et al. 2012).

Statistical Analysis

The PLS-LDA classification model, PLSR, and PCR were made using Unscrambler X 10.1 (Camo, Norway).

PLS-LDA is an extension of partial least squares (PLS). The PLS finds a set of latent variables (LVs), which are the linear combination of original independent variables (x) with the coefficient of loading weights, w. In the PLS-LDA, the response matrix is a dummy matrix containing class membership information for each sample (Aliakbarzadeh et al. 2016).

PLSR model is the most linear multivariate regression tools widely applied in spectral analysis being a quick, efficient, and optimal regression method based on covariance (Chen et al. 2014). It is particularly useful when we need to predict a set of dependent variables from a very large set of independent variables (e.g., predictors) (Abdi 2003). For a better performance of the model, a great number of factors is necessary unless the PLS model complexity and stability are weakened.

The PCR is an effective regression model which can extract feature representations from collinear and high-dimension data (Yuan et al. 2016). As in the case of PLSR, it is particularly useful when there is the need to predict a set of dependent variables from a very large set of independent variables (e.g., predictors); for a better performance of the model, a great number of factors is necessary unless the PLS model complexity and stability are weakened.

The performance of each model has been evaluated according to three parameters like the root mean square error of cross-validation (RMSECV), the root mean square error of

prediction (RMSEP), and the regression coefficient. The RMSECV was calculated using the following Eq. 1:

$$RMSECV = \sqrt{\frac{\sum_{i=1}^{n_c}(y_{est}-y_{ref})^2}{n_c}} \quad (1)$$

where n_c is the number of samples in the calibration set, y_{ref} is the reference measurement value of the sample i, and y_{est} is the estimated value for the sample i by the model constructed when the sample I is removed. The numbers of factors were determined according to the lowest RMSECV.

The RMSEP was calculated using the Eq. 2:

$$RMSEP = \sqrt{\frac{\sum_{i=1}^{n_p}\left(y_{est,p}-y_{ref,p}\right)^2}{n_p}} \quad (2)$$

where n_p is the number of samples in the prediction set, $y_{ref,p}$ is the reference measurement value of the prediction sample i, and $y_{est,p}$ is the estimated value of the model for prediction sample i.

Results and Discussion

Raman Spectra of Authentic Honey

Raman spectra of a honey analyzed (raw spectra and normalized ones) are shown in Fig. 1; each spectrum corresponds to a honey of a different botanical origin. The spectra are presented between 250 and 2400 cm^{-1}. Of the entire Raman spectrum, only the part between 250 and 1300 cm^{-1} has been used for interpretation as only here the spectral information is relevant. The region between 1300 and 2400 cm^{-1} has been eliminated because using the auto-scaling the noise might be amplified and influenced negatively the prediction. According to the Fig. 1, authentic honey presents some characteristic bands around: 346 cm^{-1} (endocyclic δ(C-C-C) ring mode of glucose covered the band at 353 cm^{-1}, which originated from the δ(C-C-C) furanoid form of fructose), 408 cm^{-1} (glucose spectrum), 498 cm^{-1} (skeletal stretching), 606 cm^{-1} (fructose spectrum), 681 cm^{-1} (stretching of CO and CCO, OCO bending), 793 cm^{-1} (glucose spectrum), 845 cm^{-1} (glucose spectrum), 1048 cm^{-1} (the band is thought to be originated from the ν(C-O) vibration of the glucose ring seen in glucose, maltose, and sucrose spectra), 1054 cm^{-1} (the vibration might be caused by a major contribution by the bending vibration of C(1)-H and COH in carbohydrates and a minor contribution by the vibration of C-N bond in proteins and amino acids), and 1238 cm^{-1} (vibration of C(6)-OH and C(1)-OH) (Corvucci et al. 2015; Li et al. 2017; Özbalci et al. 2013).

Raman Spectra of Adulterated Honey

Different Raman spectra of a polyfloral honey adulterated with fructose (F), glucose (G), inverted sugar (IS), and hydrolyzed inulin syrup (IN) in different percentages, 5, 10, 20, 30, 40, and 50%, respectively, are shown in the Fig. 2.

The honey adulterated with fructose exhibited a higher intensity of Raman spectra at 606 cm^{-1} (see Fig. 2) (skeletal intensity), 750–850 cm^{-1} (ring vibrations and C-OH stretch), and 1074 cm^{-1} (C-O-C cyclic alkyl ethers). All these wavenumbers are specific to fructose (Corvucci et al. 2015; Li et al. 2017; Özbalci et al. 2013). In contrast with the honey adulterated with fructose, glucose as an adulteration agent registered a decrease in the Raman intensity at 606, 750–850, and

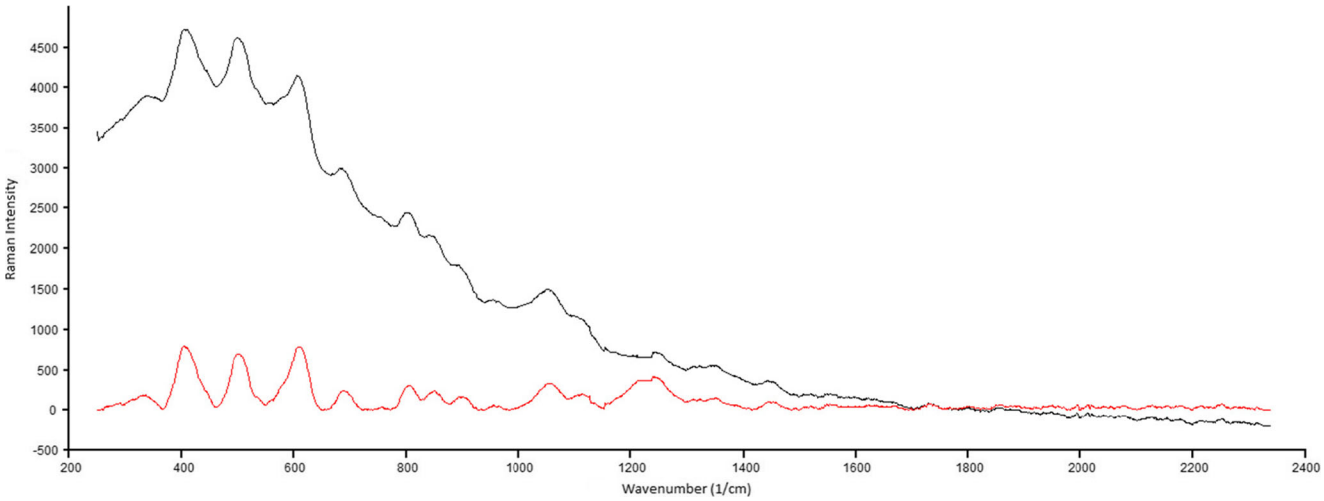

Fig. 1 Honey Raman spectra. Black line—raw spectra, red line—corrected spectra (color figure online)

1074 cm^{-1} (Fig. 2), while at wavenumbers specific to glucose the intensity increased: 498 cm^{-1} (skeletal stretching) and 918 cm^{-1} (CH, COH bend).

In the case of honey adulterated with hydrolyzed inulin syrup, it can be observed in the first moment that at 606 cm^{-1}, the intensity of the peak is increasing with the increase in the concentration of hydrolyzed inulin syrup added; this fact is normal because the inulin syrup has a high concentration of fructose and the 606 cm^{-1} is characteristic to fructose. Other bands which are characteristics of hydrolyzed inulin syrup presented an increase in their magnitude: 450 cm^{-1}—skeleton vibration, 680 cm^{-1}—deformation vibrations of the ring, 793 cm^{-1}—ring vibration, 1048 cm^{-1}—C-O-C cyclic in alkyl ethers, and 1253 cm^{-1}—C-O-C cyclic in alkyl ethers (Goodacre et al. 2002).

The honey adulterated with inverted sugar did not show high differences from the authentic samples (glucose and fructose are in the same amount in inverted sugar), but there can be observed an increase in the Raman intensity at 681 cm^{-1} (stretching of CO and CCO, OCO bending)—specific to fructose—and at 793 cm^{-1} (ring vibration)—specific to glucose spectrum (Corvucci et al. 2015; Li et al. 2017; Özbalci et al. 2013).

The malt wort spectra are not very well defined because at high concentration, the must appears like an opaque substance; however, there can be observed an increase in intensity at 470 cm^{-1} (skeletal vibration) specific to maltose. The adulteration of honey with malt wort can be made only for honeydew honey, because in the case of other honeys, color is changing too much and they can be considered only honeydew honeys; however, this is not a problem since honeydew is in great demand and the quantities are not very high at international level.

PLS-LDA—Original and Adulterated

The PLS-LDA model was used for the discrimination of authentic and adulterated honey (with hydrolyzed inulin syrup, malt must, glucose, and inverted sugar, respectively). All the 956 samples were submitted to calibration and cross-validation. The results of the model are shown in the Table 1. A correct classification of 98.53% of the samples has been observed in the case of the original validation, while in the case of the cross-validation, a correct classification of 96.54% of the samples was observed. The reason for which some authentic samples are classified as adulterated ones is due to honey composition which is of 70% monosaccharides (e.g., glucose and fructose) (Oroian et al. 2015). In the case of adulterated honey classified as authentic one, we consider that this wrong classification occurs in the case of small adulteration percentages (e.g., in the case of inverted sugar where the two components glucose/fructose are in the same ratio and the addition does not influence the system).

Fig. 2 Honey Raman spectra profile adulterated with different agents: F—fructose, G—glucose, IN—hydrolyzed inulin syrup, IS—inverted sugar, M—malt must

PLS-LDA of Adulterated Honey

The PLS-LDA model was used for the discrimination of honey adulterated (with hydrolyzed inulin syrup, malt must, glucose, and inverted sugar, respectively). All the 900 samples were submitted to calibration and cross-validation. The results of the model are shown in the Table 2. In the case of the calibration, a correct classification of 92.00% of the samples was observed, while in the case of the cross-validation, a correct classification of 89.99% of the samples was observed. Having in view the table data, one can notice that some samples adulterated with hydrolyzed inulin syrup are classified as sample adulterated with fructose; this can be explained by the fact that hydrolyzed inulin syrup contains fructose in high concentrations. In the case of honeys adulterated with glucose, some of them are classified as honey adulterated with inverted sugar, this fact is due to inverted sugar which contains glucose and fructose in equal concentrations. The best classification was observed in the case of malt wort (100%) which has a different composition from the other adulteration agents and the Raman spectra is very different from other adulterants.

Determination of Adulterant Agent Concentration

Honey is a complex food material, and the adulteration agents have a high degree of similarity with the authentic samples. For this reason, it is quite difficult to determine the exact amount of the adulteration agent added to the authentic sample based on spectrum. Keeping into account these findings, the concentration of the adulteration agent can be analyzed using chemometrics. Two types of linear model: partial least squares regression (PLSR) and principal component regression (PCR) were used to achieve the optimal regression model.

Calibration Models

In this paper, honey samples (acacia, tilia, sunflower, polyfloral, and honeydew) adulterated with different percentages of hydrolyzed inulin syrup, glucose, fructose, inverted

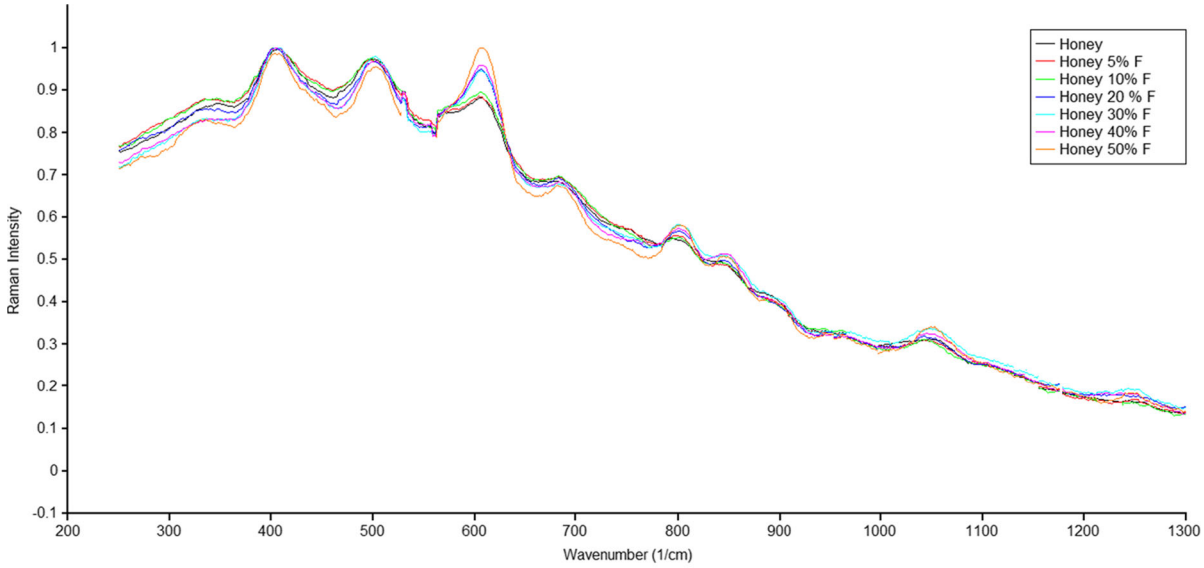
Honey
Honey 5% F
Honey 10% F
Honey 20 % F
Honey 30% F
Honey 40% F
Honey 50% F
Raman Intensity
Wavenumber (1/cm)

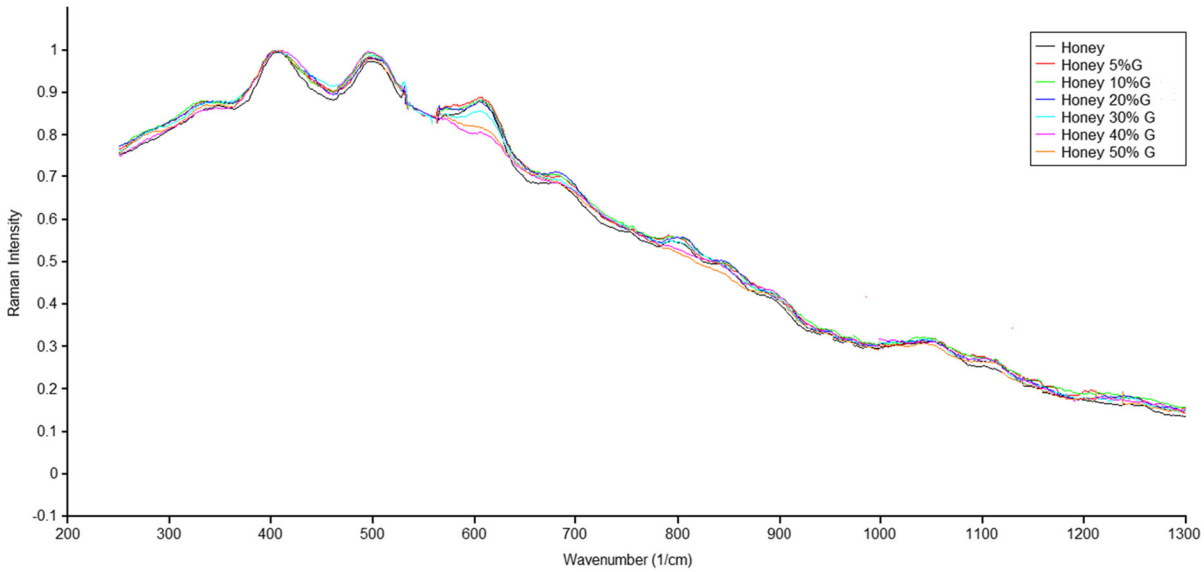
Honey
Honey 5%G
Honey 10%G
Honey 20%G
Honey 30% G
Honey 40% G
Honey 50% G
Raman Intensity
Wavenumber (1/cm)

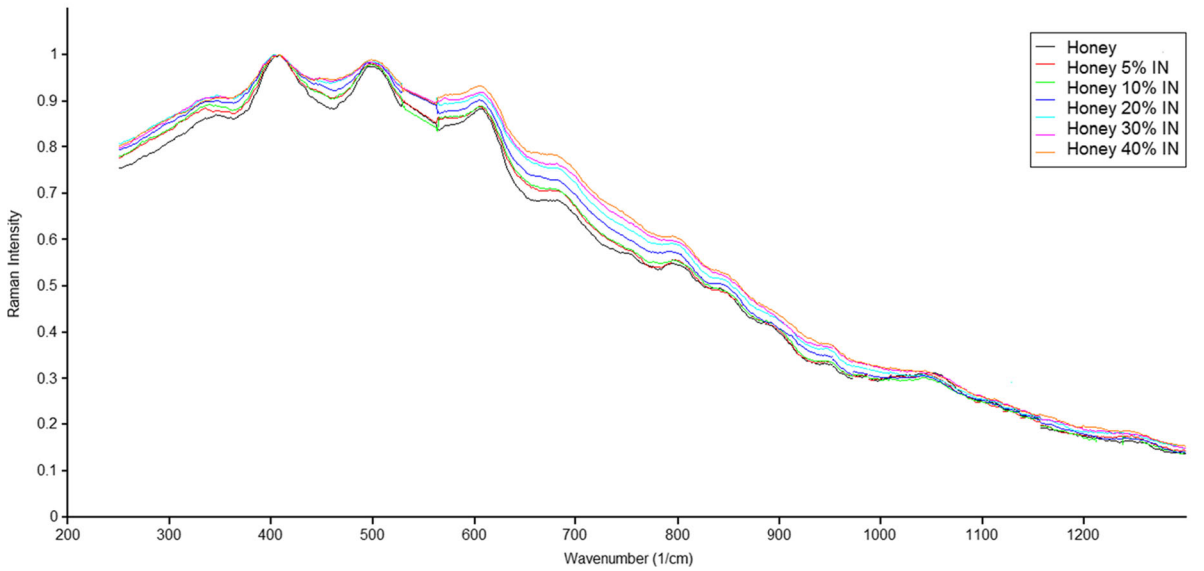
Honey
Honey 5% IN
Honey 10% IN
Honey 20% IN
Honey 30% IN
Honey 40% IN
Raman Intensity
Wavenumber (1/cm)

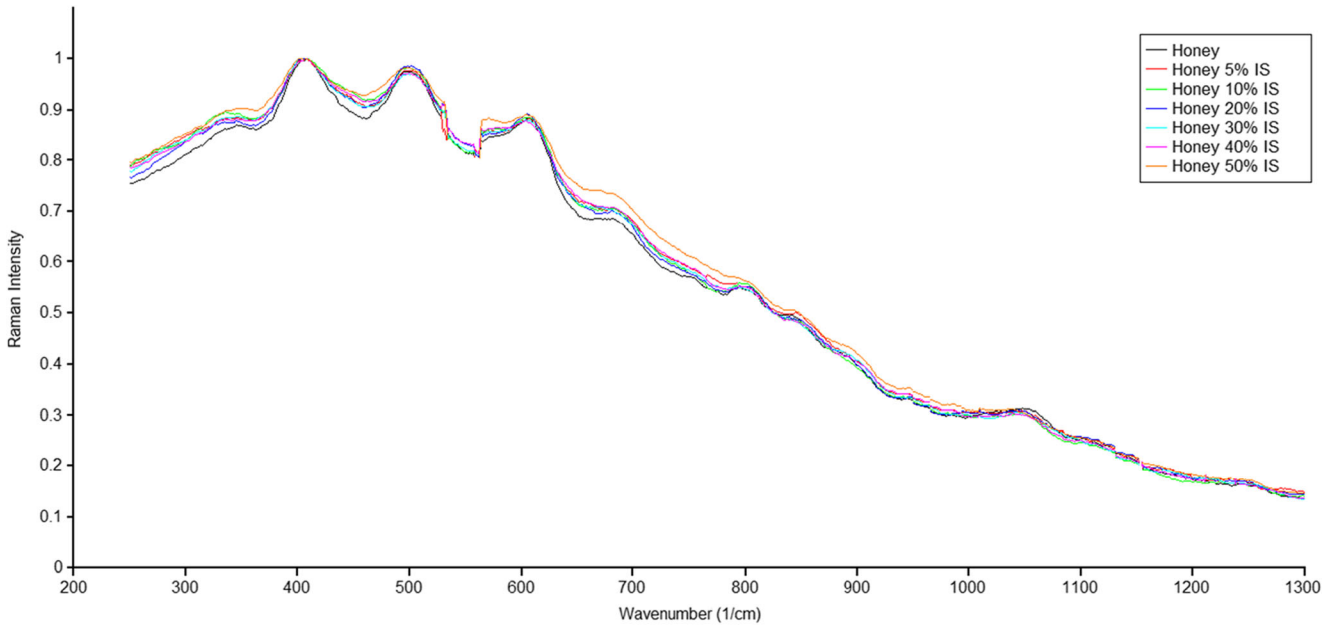

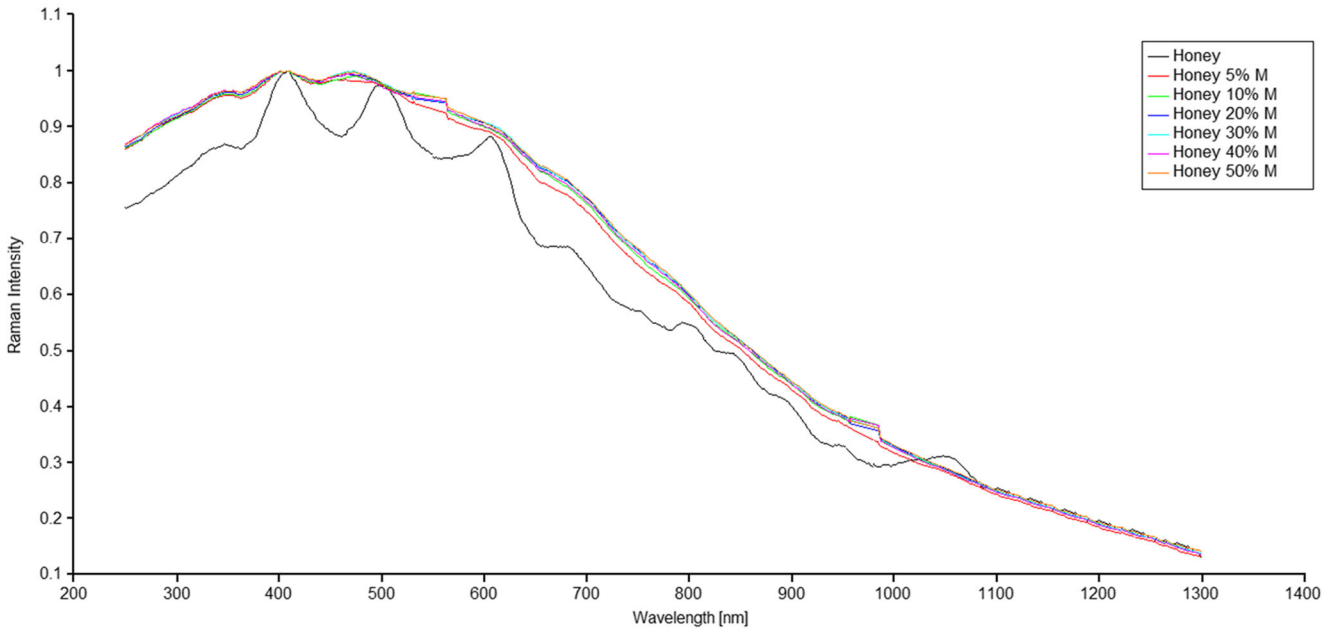

Fig. 2 (continued.)

sugar, and malt wort were used to build models. Each group (based on the adulteration agent and honey type) was used to build a model and the data were divided into two subsets: one of them is called calibration set (to build the model) and the

Table 1 Classification of honeys according to authentic or adulteration group using the PLS-LDA

Calibration					Cross-validation			
Sample	Adulterated	Authentic	Total	% correct	Adulterated	Authentic	Total	% correct
Adulterated	894	6	900	99.33	876	24	900	97.33
Authentic	8	48	56	85.71	9	47	56	83.93
Total	900	56	956	98.53	885	71	956	96.54

Table 2 Classification of honeys according to the adulteration agent using the PLS-LDA

Calibration								Cross-validation						
Sample	IN	M	G	F	IS	Total	% correct	IN	M	G	F	IS	Total	% correct
IN	162	0	0	18	0	180	90.00	162	0	0	24	0	180	90.00
M	0	180	0	0	0	180	100.00	0	180	0	0	0	180	100.00
G	0	0	156	0	24	180	86.67	0	6	150	0	24	180	83.33
F	6	0	0	174	0	180	96.67	12	0	0	168	0	180	93.33
IS	7	0	3	14	156	180	86.67	14	0	4	12	150	180	83.33
Total	175	180	159	206	180	900	92.00	188	186	154	204	174	900	90.00

IN hydrolyzed inulin syrup, *M* malt must, *G* glucose, *F* fructose, *IS* inverted sugar

Table 3 Statistical parameters of the PLSR model results in the calibration and prediction set

Adulteration agent	Honey	PCs	Calibration set		Prediction set	
			RMSECV	R^2	RMSEP	R^2
Fructose	Acacia	C8	0.001	0.998	0.012	0.972
	Honeydew	C1	0.001	0.999	0.001	0.996
	Polyfloral	C8	0.002	0.982	0.013	0.921
	Sunflower	C2	0.001	0.998	0.010	0.981
	Tilia	C11	0.002	0.992	0.012	0.911
Fructose	All	C15	0.011	0.987	0.013	0.984
Glucose	Acacia	C3	0.001	0.999	0.016	0.931
	Honeydew	C9	0.003	0.993	0.021	0.961
	Polyfloral	C5	0.001	0.999	0.005	0.956
	Sunflower	C10	0.002	0.970	0.015	0.937
	Tilia	C8	0.001	0.999	0.011	0.979
Glucose	All	C14	0.008	0.980	0.014	0.937
Inverted sugar	Acacia	C5	0.001	0.998	0.019	0.910
	Honeydew	C15	0.001	0.999	0.013	0.984
	Polyfloral	C14	0.001	0.998	0.003	0.987
	Sunflower	C7	0.004	0.929	0.019	0.915
	Tilia	C15	0.001	0.999	0.012	0.954
Inverted sugar	All	C6	0.010	0.986	0.012	0.982
Hydrolyzed inulin syrup	Acacia	C10	0.004	0.981	0.015	0.937
	Honeydew	C14	0.001	0.999	0.011	0.978
	Polyfloral	C1	0.004	0.971	0.015	0.914
	Sunflower	C3	0.001	0.993	0.015	0.948
	Tilia	C7	0.003	0.969	0.014	0.959
Hydrolyzed inulin syrup	All	C9	0.009	0.985	0.011	0.977
Malt must	Acacia	C7	0.001	0.999	0.021	0.912
	Honeydew	C11	0.003	0.994	0.012	0.982
	Polyfloral	C14	0.001	0.999	0.011	0.978
	Sunflower	C7	0.002	0.998	0.020	0.903
	Tilia	C1	0.002	0.998	0.022	0.908
Malt must	All	C15	0.004	0.991	0.005	0.984
All	All	C13	0.009	0.983	0.103	0.981

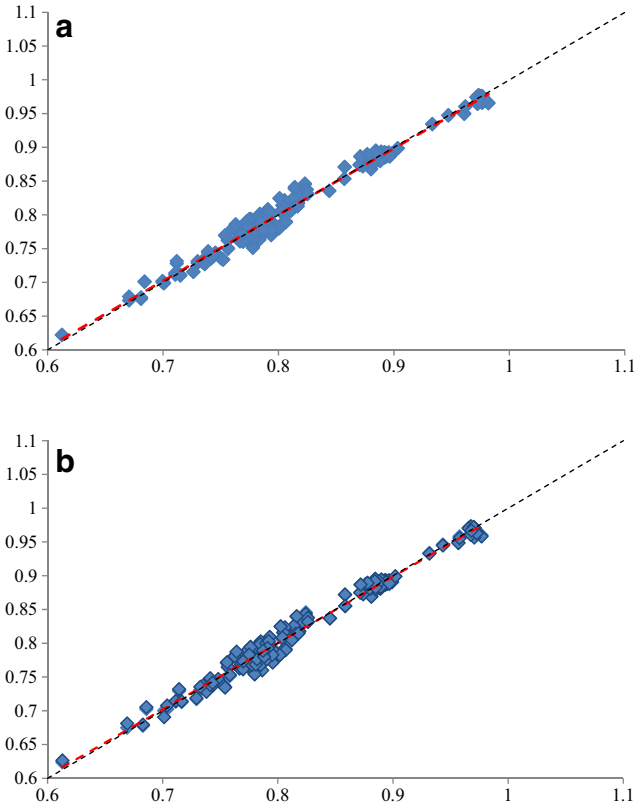

Fig. 3 Scatters plot of the mixed group models. **a** PLSR. **b** PCR. Red line—best linear fit (color figure online)

other one is to test its robustness. The data used for calibration represented two thirds of the total data, while for prediction, one third of the total data, respectively. The calibration set for each adulteration agent and honey type consisted of 29 samples, while for the prediction set consisted of 14 samples. The models were built as follows: for each adulteration agent and honey type (43 samples for each adulteration agent/honey type), the same adulteration agent and all honeys (181 samples), and all adulteration agents and all honeys (935 samples).

PLSR Model

In this study, the number of PCs for each model depending on RMSECV values using the cross-validation model has been optimized. Table 3 displays the statistical parameters of PLSR model for each honey and adulterant used. It can be observed that the number of PCs is not the same for all honeys (a number of 15 principal component (PC) has been used, out of which a suitable one has been extracted). In the case of the mixed groups, it can be observed a high number of PC (15 PC), while in the case of individual honey and adulterant agent, the number of PC ranged from 2 to 14. Accordingly to the data in the Table 3, there can be observed some differences between the RMSECV and RMSEP values, which can be explained by the number of data samples used for each type of honey.

Table 4 Statistical parameters of the PCR model results in the calibration and prediction set

Adulteration agent	Honey	PCs	Calibration set		Prediction set	
			RMSECV	R^2	RMSEP	R^2
Fructose	Acacia	C8	0.001	0.998	0.012	0.972
	Honeydew	C2	0.001	0.999	0.001	0.995
	Polyfloral	C8	0.003	0.982	0.013	0.971
	Sunflower	C10	0.002	0.992	0.013	0.975
	Tilia	C11	0.002	0.992	0.012	0.913
Fructose	All	C15	0.011	0.987	0.013	0.987
Glucose	Acacia	C3	0.001	0.999	0.016	0.932
	Honeydew	C9	0.003	0.993	0.021	0.961
	Polyfloral	C4	0.001	0.999	0.005	0.986
	Sunflower	C13	0.001	0.979	0.017	0.928
	Tilia	C8	0.001	0.999	0.011	0.979
Glucose	All	C15	0.008	0.980	0.014	0.940
Inverted sugar	Acacia	C7	0.001	0.999	0.019	0.905
	Honeydew	C15	0.001	0.999	0.013	0.984
	Polyfloral	C7	0.001	0.996	0.003	0.977
	Sunflower	C7	0.004	0.929	0.019	0.915
	Tilia	C15	0.001	0.999	0.012	0.954
Inverted sugar	All	C6	0.010	0.986	0.013	0.981
Hydrolyzed inulin syrup	Acacia	C15	0.003	0.988	0.012	0.982
	Honeydew	C14	0.001	0.999	0.011	0.978
	Polyfloral	C1	0.004	0.951	0.015	0.915
	Sunflower	C3	0.001	0.993	0.015	0.948
	Tilia	C15	0.003	0.969	0.015	0.957
Hydrolyzed inulin syrup	All	C12	0.009	0.985	0.011	0.977
Malt must	Acacia	C7	0.001	0.999	0.021	0.912
	Honeydew	C1	0.003	0.994	0.012	0.982
	Polyfloral	C14	0.001	0.999	0.011	0.978
	Sunflower	C7	0.002	0.998	0.020	0.903
	Tilia	C14	0.001	0.998	0.021	0.912
Malt must	All	C15	0.004	0.991	0.006	0.978
All	All	PC15	0.009	0.983	0.010	0.981

The experimental versus predicted data of the Raman spectra intensity are shown in the Fig. 3.

PCR

In this study, the number of PCs for each model in function of the RMSECV values using the cross-validation model has been optimized. The statistical parameters of PCR model for each honey and adulterant used are shown in the Table 4. In the case of PLSR, the number of PCs is not the same as in the case of all honeys ranging from 1 to 15; in the case of all honeys and all adulterants, the number of PC is maximum (a number of 15 PCs have been used, out of which a suitable one has been extracted). The experimental versus predicted data of the Raman spectra intensity is shown in Fig. 3.

The two types of models have been applied to all honeys irrespective of the adulterant used (see Tables 3 and 4). It can be observed that the two models have quite similar RMSE values and the regression coefficients do not have great differences. In the case of the model applied to all honeys and adulterants, the RMSE values and regression coefficients are better in the case of PCR model. According to the data presented in the tables, there can be observed that the PCR model predicts better than PLSR model in the case of individual honeys and adulterants. These results demonstrated that the model built by mixed group was not worse than those models built by the same botanical origin honey samples, but even better due to the fact that the mixed group contained the most information on honey and adulterant. It can be concluded that the samples consisting of different types of honey may be used to build the model and not to reduce its accuracy. The scattered plots with the experimental and predicted data of Raman intensity are presented in opposition in the Fig. 3; it can be observed that many points in the prediction set fall to or close to the red line (which represents the best linear fit line between the experimental and predicted data). The data falling on the red line shows that the concentration of the adulteration values by the Raman intensity spectra is equal to the experimental data.

Conclusions

Raman spectroscopy combined with PLS-LDA, PLSR, and PCR was successfully applied to detect adulterants in honey. Raman spectroscopy combined with PLS-LDA seems more successful in detecting malt wort in honey than glucose and inverted sugar. The method applied is simple and efficient, and it is appropriate for field applications as the sample does not need pre-processing. The PCR method is a good method of predicting the concentration of the adulteration agent in adulterated honey.

Funding Information Mircea Oroian, Sergiu Paduret, and Sorina Ropciuc have been financed by the National Authority for Scientific Research and Innovation, CNCS-UEFISCDI, grant number PN-II-RU-TE-2014-4-0110.

Compliance with Ethical Standard

Conflict of Interest Mircea Oroian declares that he has no conflict of interest. Sorina Ropciuc declares that she has no conflict of interest. Sergiu Paduret declares that he has no conflict of interest.

Ethical Approval Not applicable.

Research Involving Human Participants and/or Animals Not applicable.

Informed Consent Not applicable.

References

Abdi H (2003) Partial least square (PLS) regression. Encyclopedia of social sciences research methods. Thousand Oaks (CA): Sage (pp. 792-795). https://doi.org/10.4135/9781412950589.n690

Aliakbarzadeh G, Parastar H, Sereshti H (2016) Crossmark. Chemom Intell Lab Syst 158:165–173. https://doi.org/10.1016/j.chemolab.2016.09.002

Bázár G, Romvári R, Szabó A, Somogyi T, Éles V, Tsenkova R (2016) NIR detection of honey adulteration reveals differences in water spectral pattern. Food Chem 194:873–880. https://doi.org/10.1016/j.foodchem.2015.08.092

Chen Q, Qi S, Li H, Han X, Ouyang Q, Zhao J (2014) Determination of rice syrup adulterant concentration in honey using three-dimensional fluorescence spectra and multivariate calibrations. Spectrochim Acta A Mol Biomol Spectrosc 131:177–182. https://doi.org/10.1016/j.saa.2014.04.071

Çinar SB, Ekşi A, Coşkun I (2014) Carbon isotope ratio (13C/12C) of pine honey and detection of HFCS adulteration. Food Chem 157:10–13. https://doi.org/10.1016/j.foodchem.2014.02.006

Corvucci F, Nobili L, Melucci D, Grillenzoni FV (2015) The discrimination of honey origin using melissopalynology and Raman spectroscopy techniques coupled with multivariate analysis. Food Chem 169:297–304. https://doi.org/10.1016/j.foodchem.2014.07.122

Gan Z, Yang Y, Li J, Wen X, Zhu M, Jiang Y, Ni Y (2015) Using sensor and spectral analysis to classify botanical origin and determine adulteration of raw honey. J Food Eng 178:151–158. https://doi.org/10.1016/j.jfoodeng.2016.01.016

Goodacre R, Radovic BS, Anklam E (2002) Progress toward the rapid nondestructive assessment of the floral origin of European honey using dispersive Raman spectroscopy. Appl Spectrosc 56(4):521–527. https://doi.org/10.1366/0003702021954980

Guelpa A, Marini F, du Plessis A, Slabbert R, Manley M (2016) Verification of authenticity of South African honey and fraud detection using NIR spectroscopy. Food Control 73:1388–1396. https://doi.org/10.1016/j.foodcont.2016.11.002

Li S, Shan Y, Zhu X, Zhang X, Ling G (2012) Detection of honey adulteration by high fructose corn syrup and maltose syrup using Raman spectroscopy. J Food Compos Anal 28(1):69–74. https://doi.org/10.1016/j.jfca.2012.07.006

Li S, Zhang X, Shan Y, Su D, Ma Q, Wen R, Li J (2017) Qualitative and quantitative detection of honey adulterated with high-fructose corn syrup and maltose syrup by using near-infrared spectroscopy. Food Chem 218:231–236. https://doi.org/10.1016/j.foodchem.2016.08.105

Oroian M (2012) Physicochemical and rheological properties of Romanian honeys. Food Biophys 7(4):296–307. https://doi.org/10.1007/s11483-012-9268-x

Oroian M (2015) Influence of temperature, frequency and moisture content on honey viscoelastic parameters—neural networks and adaptive neuro-fuzzy inference system prediction. LWT Food Sci Technol 63(2):1309–1316. https://doi.org/10.1016/j.lwt.2015.04.051

Oroian M, Amariei S, Rosu A, Gutt G (2015) Classification of unifloral honeys using multivariate analysis. J Essent Oil Res 27(6):533–544. https://doi.org/10.1080/10412905.2015.1073183

Owen CA, Notingher I, Hill R, Stevens M, Hench LL (2006) Progress in Raman spectroscopy in the fields of tissue engineering, diagnostics and toxicological testing. J Mater Sci Mater Med 17:1019–1023. https://doi.org/10.1007/s10856-006-0438-6

Özbalci B, Boyaci IH, Topcu A, Kadilar C, Tamer U (2013) Rapid analysis of sugars in honey by processing Raman spectrum using chemometric methods and artificial neural networks. Food Chem 136(3–4):1444–1452. https://doi.org/10.1016/j.foodchem.2012.09.064

Shafiee S, Polder G, Minaei S, Moghadam-Charkari N, Van Ruth S, Kuś PM (2016) Detection of Honey Adulteration using Hyperspectral Imaging. IFAC-PapersOnLine 49(16):311-314. https://doi.org/10.1016/j.ifacol.2016.10.057

Simsek A, Bilsel M, Goren AC (2012) 13C/12C pattern of honey from Turkey and determination of adulteration in commercially available honey samples using EA-IRMS. Food Chem 130(4):1115–1121. https://doi.org/10.1016/j.foodchem.2011.08.017

Wang S, Guo Q, Wang L, Lin L, Shi H, Cao H, Cao B (2015) Detection of honey adulteration with starch syrup by high performance liquid chromatography. Food Chem 172:669–674. https://doi.org/10.1016/j.foodchem.2014.09.044

Yuan X, Huang B, Ge Z, Song Z (2016) Double locally weighted principal component regression for soft sensor with sample selection under supervised latent structure. Chemom Intell Lab Syst 153:116–125. https://doi.org/10.1016/j.chemolab.2016.02.014

Zhu X, Li S, Shan Y, Zhang Z, Li G, Su D, Liu F (2010) Detection of adulterants such as sweeteners materials in honey using near-infrared spectroscopy and chemometrics. J Food Eng 101(1):92–97. https://doi.org/10.1016/j.jfoodeng.2010.06.014